Reactive Extrusion: Toward Nanoblends

Guo-Hua Hu* and Hervé Cartier†

Laboratoire des Sciences du Génie Chimique, Ecole Européenne d'Ingénieurs en Génie des Matériaux, CNRS-ENSIC-INPL, 1 rue Grandville, B.P. 451, 54001 Nancy Cedex, France

Christopher Plummer

Laboratoire de Polymères, Département des Matériaux, Ecole Polytechnique Fédérale de Lausanne, 1015 Lausanne, Switzerland

Received December 15, 1998; Revised Manuscript Received April 13, 1999

ABSTRACT: By nanoblends, it is meant that the scale of dispersion of one polymer phase in the other is below 100 nm. A novel method was developed to prepare nanostructured blends (nanoblends) of polypropylene (PP) and polyamide-6 (PA-6) directly in a screw extruder. It consisted of polymerizing a monomer of PA-6, ϵ-caprolactam (ϵ-CL), in the matrix of PP. A fraction of the latter bore 3-isopropenyl-α,α-dimethylbenzene isocyanate (TMI) which acted as growing centers to initiate PA-6 chain growth. As such, formation of PA-6 and a graft copolymer of PP and PA-6 took place simultaneously in the matrix of the PP, leading to compatibilized PP/PA-6 blends. The size of the particles of the dispersed phase (PA-6) was between 10 and 100 nm, which could not be achieved otherwise by melt blending premade PP and PA-6.

Introduction

Over the past two decades, blending existing polymers in a polymer processing machine such as a screw extruder has proven to be very successful for obtaining new materials at reduced costs. It has been learnt that the ultimate properties of such multiphasic materials depend very much on the morphology of such systems and the interfacial adhesion between phases. The morphology is dictated primarily by the flow type, the viscosity ratio, and the capillary number (Ca).[1,2] This latter is defined as the ratio between shear stress the flow field imposed to the particles which tends to deform and/or break them up and the interfacial stress which opposes to this deformation and/or breakup:

$$Ca = \frac{\text{shear stress}}{\text{interfacial stress}} = \frac{\eta_m \dot{\gamma} d}{\sigma}$$

η_m is the viscosity of the matrix, $\dot{\gamma}$ the shear rate, d the diameter of the particles, and σ the interfacial tension. To some extent, the ultimate particle size results from the competition between thermomechanics ($\eta_m\dot{\gamma}$) and thermodynamics (σ). Conceptually, this can be represented in Figure 1a. When a mixture of two polymers is subjected to a flow field, particles of the dispersed phase reduce in size along the flow stream and become less and less deformable. A threshold will be reached when a dynamic equilibrium is established between thermomechanical and thermodynmic forces. At this point, the particles can no longer be deformed and their breakup will become impossible. In practice, an interfacial emulsifier, which is often a block or graft copolymer, is added or generated in situ during blending. Its roles are to reduce the interfacial tension, help dispersion and more importantly stabilize the system by preventing particles from coalescing—compatibilization. It has been shown experimentally by many authors that for most polymer blends processed under typical extrusion conditions, the particle size of the dispersed phase is rarely below 0.1 μm (or 100 nm) whatever the compatibilization method employed.[3−5]

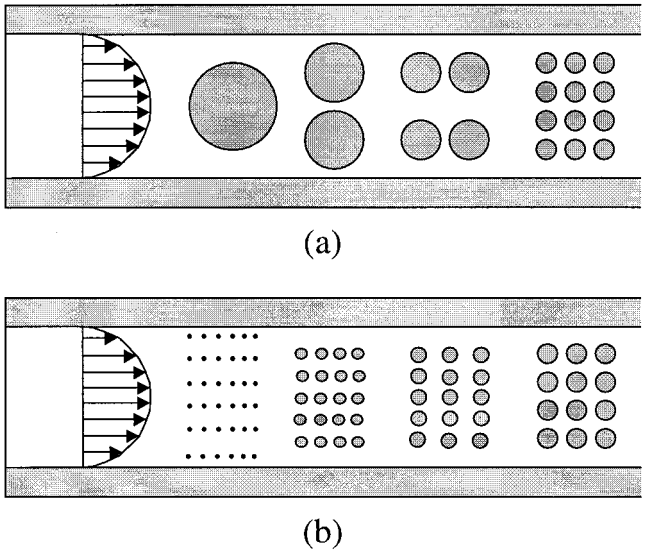

Figure 1. Schematic representation of the mechanisms of the morphology development of two different systems subjected to a flow field in a tube. (a) An immiscible mixture of polymer A and polymer B; (b) a mixture of a polymer and a polymerizable monomer.

Then two questions arise. Would a finer dispersion of the order of, say, 10−100 nm (nanodispersion) bring additional benefits to such multiphasic materials? If yes, how would this level of dispersion be reached? To answer these two questions, instead of melt blending existing polymers, we developed a concept that consisted in polymerizing the monomer of one of the polymers in the presence of the other.[6] The process of the morphology development can be schematically depicted in

* To whom correspondence should be addressed. Tel: +33-383-17-53-39; Fax: +33-383-17-51-55; E-mail: hu@ensic.u-nancy.fr.
† Present address: General Electric Plastics, Bergen op Zoom, The Netherlands.

10.1021/ma981924y CCC: $18.00
Published on Web 06/18/1999

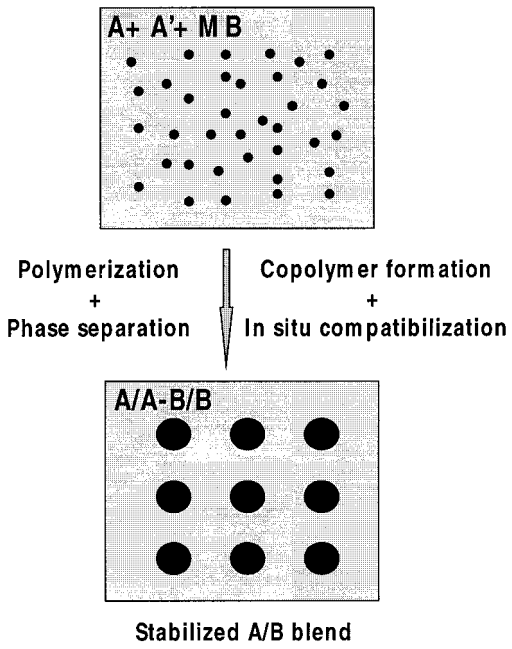

Figure 2. Schematic description of the in situ polymerization and in situ compatibilization method for preparing nanoblends.

Figure 1b. For the sake of simplicity, consider a homogeneous mixture of a polymer (A) and a polymerizable monomer (MB) subjected to a flow field. Prior to polymerization, the system is monophasic. It becomes phase separated as polymerization proceeds if the resulting polymer B is immiscible with polymer A. Meanwhile the size of the particles of polymer B increases. If there is no interfacial emulsifier present in the system, the resulting blend will not be very different from one that would be obtained by melt blending premade polymer A and polymer B, whose morphology will be gross and unstable. However, if a fraction of polymer A chains bear initiating sites either at the chain end(s) or along the chains, denoted here as A′, from which polymer B chains can grow, then formation of both polymer B and an A−B copolymer takes place simultaneously. In fact, four phenomena are involved in the process (Figure 2): polymerization of MB which produces polymer B and causes phase separation and eventually phase inversion; formation of an A−B copolymer that stabilizes the system. For this reason, we call the method in situ polymerization and in situ compatibilization of polymer blends. Conceptually, it should allow to obtain a variety of morphology including nanodispersion of one polymer in the other upon controlling the kinetics of polymerization, phase separation, and copolymer formation. In the case of nanodispersion, both the amount and the rate of formation of the copolymer should be sufficiently high compared with the rates of polymerization and phase separation so that the morphology can be stabilized in the early stage of the phase separation.

In this paper, we show the potential of the in situ polymerization and in situ compatibilization described above using polypropylene (PP) and polyamide-6 (PA-6) blends as example. We polymerize anionically ϵ-caprolactam (ϵ-CL) in the presence of PP using a catalyst and an activator. A fraction of the PP chains bear isocyanate groups which act as growing centers to initiate PA-6 chain growth from PP chains to form a graft copolymer of PP and PA-6. In this way, we obtain compatibilized PP/PA-6 blends of varying composition and morphology, some of which could not be obtained otherwise by melt blending premade PP and PA-6.

The Underlying Chemistry of in Situ Polymerized and in Situ Compatibilized PP/PA-6 Nanoblends

Polyamide-6 (PA-6) can be synthesized by activated anionic polymerization of ϵ-caprolactam (ϵ-CL) in the presence of a catalyst (sodium caprolactamate, NaCL) and an activator. This latter is typically an ester or isocyanate-bearing compound. The reaction mechanism using an isocyanate (R−N═C═O) as an activator is described in (Figure 3).[7,8] Basically, polymerization starts with the formation of an acyl caprolactam as a result of the reaction between R−N═C═O and ϵ-CL (reaction 1). This acyl caprolactam then reacts readily with NaCL forming a new reactive sodium salt (reaction 2). This latter initiates the polymerization of ϵ-CL; meanwhile the catalyst (NaCL) is restored (reaction 3). Repetition of reactions 2 and 3 finally leads to a high molecular weight PA-6 (reactions 4 and 5). As opposed to the hydrolytic polymerization of PA-6 which requires several hours, the activated anionic polymerization of ϵ-CL can be accomplished in a few minutes or less. This time range is compatible with the residence time in a screw extruder. [9−12]

If ϵ-CL is polymerized in the presence of PP, a highly immiscible mixture of PP and PA-6 will be obtained. Its morphology is expected to be the same as or similar to that obtained by simply blending premade PP and PA-6. If a fraction of PP contains isocyanate moieties along the chains, a graft copolymer of PP and PA-6 will be formed as well. This is because according to reactions 1 and 2, acyl caprolactam as a result of the reaction of isocyanate-bearing PP with ϵ-CL acts as growing centers for the polymerization of ϵ-CL (Figure 4).

The use of an acrylate-bearing PP in place of an isocyanate-bearing PP should also lead to the formation of a graft copolymer. For example, pure polyethylene−PA-6 graft copolymers and polystyrene−PA-6 graft copolymers were obtained using ethylene−ethyl acrylate copolymers and styrene−acrylate copolymers as activators, respectively.[13,14] In this study, PP bearing 3-isopropenyl-α,α-dimethylbenzene isocyanate (TMI) was used as macro-activator, denoted as PP-*g*-TMI. Unlike classical isocyanates, TMI is sufficiently stable under extrusion conditions (high temperatures and exposure to moisture). It should be noted that previous works reported in the literature aimed at either synthesizing pure graft copolymers with PA-6 grafts by polymerizing ϵ-CL onto an acrylate bearing polymer backbone[13,14] or preparing polymer blends by polymerizing ϵ-CL in the presence of another polymer (PP).[12] In this latter case, no macromolecular activator was used and thus no copolymer was formed to stabilize the morphology of the blends. The novelty of the present study lies in the simultaneous formation of PA-6 and a graft copolymer of PP and PA-6 in the PP matrix, forming therefore well stabilized PP/PA-6 nanoblends.

Experimental Section

Materials. The polypropylene (PP) used in this study had number- and weight-average molecular weights of 62 000 and 280 000 g/mol, respectively. The monomer (ϵ-CL), the catalyst (NaCL), and the microactivator (ϵ-caprolactam blocked hexamethylene diisocyanate) were kindly supplied by DSM, The Netherlands. The catalyst contained 1.4 mol of Na per kg of ϵ-CL and the activator 2.0 mol of isocyanate per kg of ϵ-CL.

Initiation:

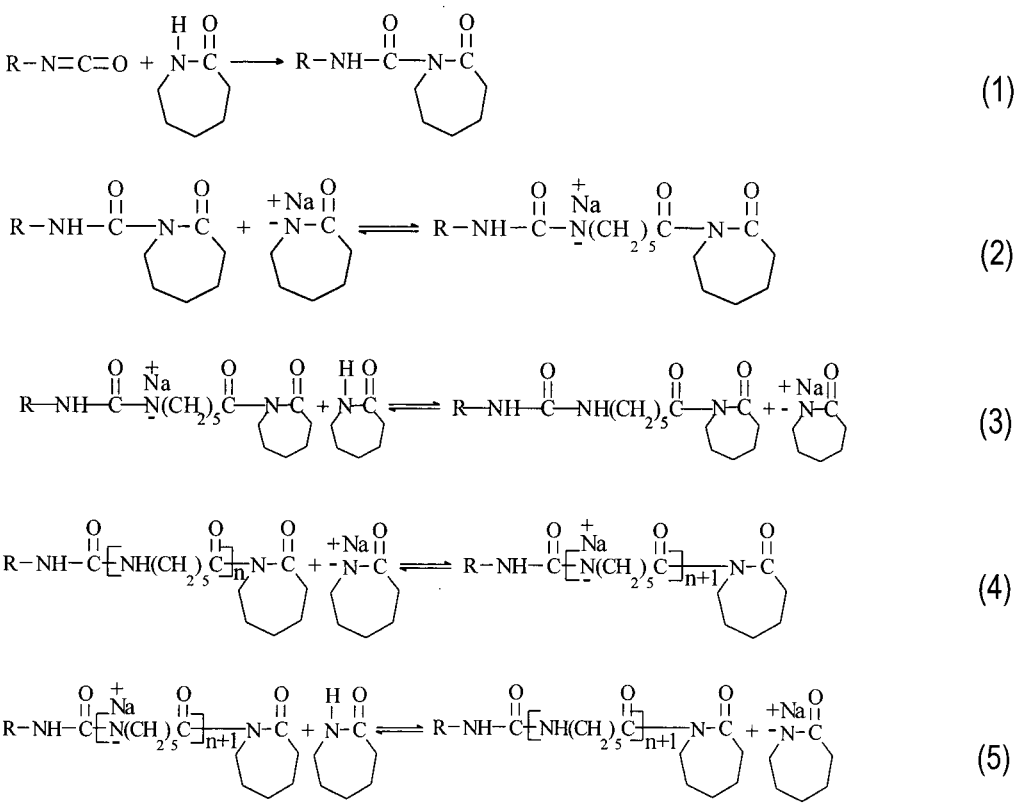

Propagation:

Figure 3. Schematic description of the activated anionic polymerization of ϵ-CL.

Initiation involving an isocyanate bearing PP:

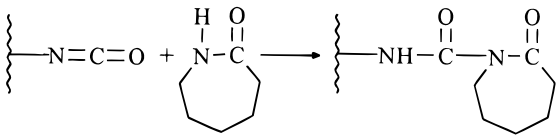

Expected structure of the copolymer of PP and PA-6 formed:

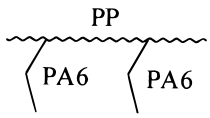

(7)

Figure 4. Mechanism of formation of a graft copolymer of PP and PA-6 using an isocyanate-bearing PP as macromolecular activator.

The macro-activator (PP-*g*-TMI) was prepared in our laboratory[15] and contained 1.1 wt % TMI. Its number- and weight-average molecular weights were 45 000 and 121 000 g/mol, respectively.

Preparation of PP/PA-6 Blends. A corotating self-wiping twin screw extruder of type Werner Pfleiderer ZSK-30 was used for preparing the PP/PA-6 blends. Since the chemistry involved was an anionic polymerization which is moisture sensitive, the PP pellets were dried at 80 °C under hot air circulation for about 4 h and the PP-*g*-TMI pellets were dried at 120 °C in a vacuum oven overnight. All extrusion experiments were carried out under constant nitrogen purge. The barrel temperature profile was 200 °C between the hopper and the first kneading zone and 240 °C for the rest of the screw length. All components involved in the polymerizing system (PP, PP-*g*-TMI, ϵ-CL, NaCL, and the microactivator) were fed together to the extruder through the main hopper. To better illustrate the performance of the concept of in situ polymerization and in situ compatibilization with respect to classical melt blending, two polymerizing systems were investigated: PP/ϵ-CL/NaCL/microactivator (50/50/3/3 by weight) and PP-*g*-TMI/ϵ-CL/NaCL/microactivator (50/50/3/3 by weight). The compositions of the final PP/PA-6 blends would be very close to 50/50 by weight, which are known to be most difficult to compatibilize.

Characterization of PP/PA-6 Blends. The morphology of the blend resulting from the PP/ϵ-CL/NaCL/microactivator (50/50/3/3) system was characterized by scanning electron microscopy (SEM) and that from the PP-*g*-TMI/ϵ-CL/NaCL/microactivator (50/50/3/3) by transmission electron microscopy (TEM). Prior to SEM observation, the blend was fresh fractured and then subjected to formic acid treatment at room temperature overnight under mild stirring to remove the dispersed phase (PA-6). The surface of the fractured sample was then gold-sputtered. The procedure for the TEM analysis was standard. The samples were mounted in an epoxy resin as a support and an internal surface exposed using a diamond knife at about −100 °C. They were then immersed in aqueous RuO_4 overnight (prepared by adding 200 mg of $RuCl_3 \cdot 3H_2O$ to 10 mL of 5% aqueous NaClO) and dried under vacuum. Thin sections (between 70 and 100 nm) were prepared at room temperature using a 45° diamond knife and the Reichart-Jung Ultracut-E Ultrmicrotome. The elongation at break of those blends was also measured using a tensile machine.

Results

Compositions of the Polymerized Systems. The materials obtained from the polymerization of the PP/ϵ-CL/NaCL/microactivator (50/50/3/3) and PP-*g*-TMI/ϵ-CL/NaCL/microactivator (50/50/3/3) systems were sub-

Table 1. Selected Characteristics of the Blends Obtained from PP/ϵ-CL/NaCL/Microactivator (50/50/3/3) and PP-*g*-TMI/ϵ-CL/NaCL/Microactivator (50/50/3/3) Polymerizing Systems, Respectively

	PP/ϵ-CL/NaCL/microactivator (50/50/3/3)	PP-*g*-TMI/ϵ-CL/NaCL/microactivator (50/50/3/3)
PP/PA-6	51/49	51/49
PP-*g*-PA-6	0	70.7
PP/PA-6 in PP-*g*-PA-6		70/30 (acetone extraction) 69.7/30.3 (elem anal.)
no. of PA-6 grafts per PP	0	2.5
$\bar{M}_n$ of each PA-6 graft	0	8200 g/mol

jected to several analyses. The conversions of ϵ-CL were determined by measuring the weight loss of given amounts of polymerized materials before and after solvent extraction in boiling acetone. They were about 96% for both polymerizing systems, indicating that both blends contained 51 wt % PP and 49 wt % PA-6. The first blend was composed of two distinct polymers (PP and PA-6) whereas the second one a graft copolymer (PP-*g*-PA-6) and a homopolymer (PA-6). In other words, the first blend was of type A/B and the second one A−B/B.

The amount of the PA-6 homopolymer in the second blend was determined by solvent extraction in formic acid at room temperature and was found to be 29.3 wt %. This implies that the PA-6 in the form of the PP-*g*-PA-6 graft copolymer was 19.7 wt %. Since the PP-*g*-PA-6/PA-6 blend contained 51 wt % PP and 49 wt % PA-6, the weight percentage of the PP-*g*-PA-6 in the blend would be 70.7 wt %, of which the PP and PA-6 segments were 70 and 30 wt %, respectively. The composition of the graft copolymer was also determined by elemental analysis based on nitrogen, which amounted to 3.75 wt %. This means that the graft copolymer was composed of 69.7 wt % PP and 30.3 wt % PA-6, which was in excellent agreement with the results obtained by the solvent extraction in formic acid.

Since the PP-*g*-TMI used contained 1.1 wt % TMI and had a number-average molecular weight of 45 000 g/mol, there were, on the average, 2.5 TMI moieties per PP-*g*-TMI chain. If all TMI moieties participated in the formation of the PP-*g*-PA-6 graft copolymer, then each PP backbone would bear, on the average, 2.5 PA-6 grafts—this is of course a crude representation of the real situation because the actual number of TMI per PP was unknown and difficult to determine. Thus the number-average weight of a single PA-6 graft would be about 8 200 g/mol based on the composition of the graft copolymer determined by the elemental analysis. For the sake of clarity, the above-mentioned characteristics of the two polymerizing systems after polymerization are tabulated in Table 1.

Morphology of the Polymerized Systems and the PP-*g*-PA-6 Graft Copolymer. As shown in Figure 5a, the morphology of the PP/PA-6 (51/49) blend obtained from the polymerization of the PP/ϵ-CL/NaCL/microactivator (50/50/3/3) was very gross. The average size of the PA-6 particles was as big as 200 μm. This is a typical morphology of a blend of two immiscible polymers whose compositions are close to 50/50. By contrast, the morphology of the PP-*g*-PA-6/PA-6 (70.7/29.3) blend resulting from the polymerization of the PP-*g*-TMI/ϵ-CL/NaCL/microactivator (50/50/3/3) was extremely fine (Figure 5b). The average PA-6 particle size was as small as 80 nm. This nanodispersion could not be achieved otherwise by melt blending 51 wt % PP and 49 wt % PA-6, whatever the compatibilization method employed (in situ compatibilization by replacing partly or totally the PP with a maleic anhydride modified PP or ex situ compatibilization by adding an interfacial emulsifier synthesized separately). The TEM photo also shows the preferential location of the PP-*g*-PA-6 graft copolymer at the interfaces as revealed clearly by a black layer surrounding each PA-6 particle. Figure 5c shows the microstructure of the pure PP-*g*-PA-6 graft copolymer. The PA-6 grafts were organized in lamella as revealed by the hairlike gray areas in the TEM photo.

Mechanical Properties of the Polymerized Systems. The elongation at break of the specimens of both systems after polymerization was measured by an Instron instrument following ASTM 638-71A. For the standard testing speed of 50 mm/min, the specimens of the blend from the PP/ϵ-CL/NaCL/ microactivator (50/50/3/3) were very brittle, as expected (Figure 6). Their elongation at break was less than 10%. By contrast, the specimens of the blend obtained from the PP-*g*-TMI/ϵ-CL/NaCL/microactivator (50/50/3/3) displayed a very ductile behavior at the same testing speed. They did not break down within the span of the testing machine used (250%). This was so even when the testing speed was increased to 150 mm/min. At a testing speed of 500 mm/min, which was 10 times higher than the standard testing speed, the specimens still had an elongation at break of 142%. This is truly remarkable for an immscible polymer blend especially for a composition close to 50/50.

Discussion

Using two different systems, PP/ϵ-CL/NaCL/microactivator (50/50/3/3 by weight) and PP-*g*-TMI/ϵ-CL/NaCL/microactivator (50/50/3/3 by weight), we have shown for the first time that nanodispersion of the order of 10−100 nm can be reached by in situ polymerization and in situ compatibilization. Moreover, this level of dispersion does bring additional benefits to multiphasic materials, at least for PP/PA-6 blends.

As outlined in the Introduction, the underlying mechanisms of the morphology development are very different between the classical melt reactive blending and the in situ polymerization and in situ compatibilization process. In the former case, morphology is generated by reducing the size of the dispersed phase in the matrix. In the latter case, it is formed by polymerization-induced phase separation. This explains in part the fact that the classical melt reactive blending usually cannot reach a level of dispersion below 100 nm.

The mechanisms of copolymer formation are also different between the above two approaches. This is schematically illustrated in Figure 7. For the PP-*g*-MA (maleic anhydride modified PP)/PA-6 reactive blending system, the interfacial region surrounding a PA-6 particle is composed of the PP-*g*-MA and PA-6 bearing a terminal amine group. Their reaction at the interfaces leads to the formation of a graft copolymer of PP and PA-6. The amount of copolymer formed by this method

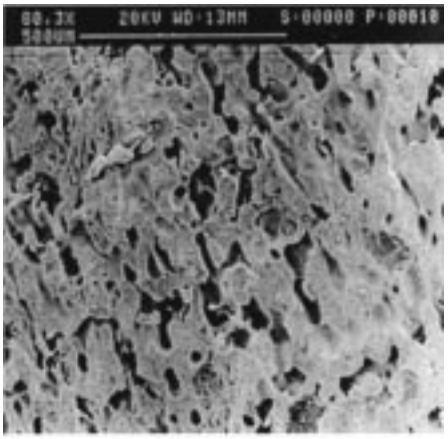

(a)

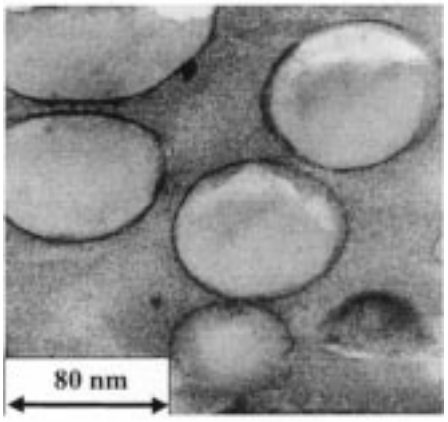

(b)

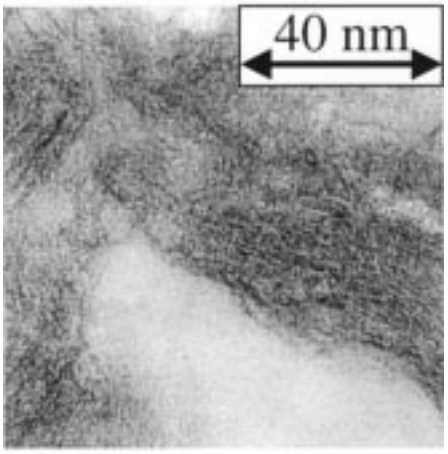

(c)

Figure 5. Morphology of the polymerized PP/ϵ-CL/NaCL/microactivator (a) and PP-*g*-TMI/ϵ-CL/NaCL/microactivator (b) systems and that of the pure PP-*g*-PA-6 graft copolymer (c).

is limited primarily by the total interfacial volume,[16] which is very small compared to the bulk. The situation is very different for the PP-*g*-TMI/ϵ-CL/NaCL/microactivator system. Being immiscible with the PP-*g*-TMI, the mixture of ϵ-CL/NaCL/microactivator is in the form of fine droplets in the PP-*g*-TMI. The interfacial region surrounding a droplet of ϵ-CL/NaCL/microactivator is PP-*g*-TMI/ϵ-CL/NaCL. The polymerization of ϵ-CL occurs in these droplets leading to PA-6 particles, which

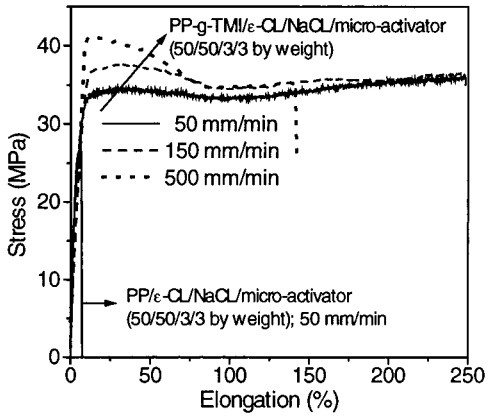

Figure 6. Stress−strain traces of the blend prepared from the PP-*g*-TMI/ϵ-CL/NaCL/microactivator (50/50/3/3) system at different testing speeds. Testing speed = 50 (solid line), 150 (dashed line), and 500 mm/min (dotted line). The stress−strain curve for the blend prepared from the PP/ϵ-CL/NaCL/microactivator (50/50/3/3) system was also shown for comparison; testing speed = 50 mm/min (solid line).

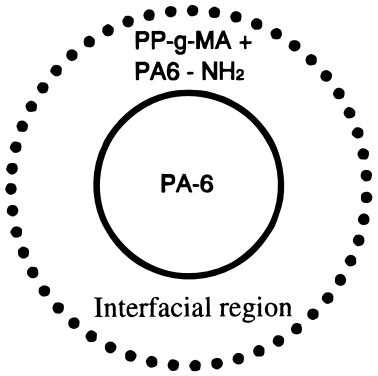

(a)

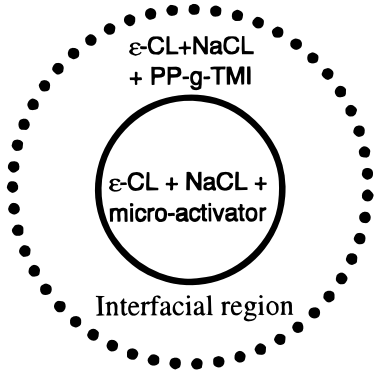

(b)

Figure 7. Comparison of the mechanism of copolymer formation between a PP-*g*-MA/PA-6 reactive blending system (a) and a PP-*g*-TMI/(ϵ-CL + NaCL + microactivator) in situ polymerizing and in situ compatibilizing system (b).

are stabilized by a layer of the graft copolymer resulting from the polymerization of PP-*g*-TMI/ϵ-CL/NaCL in the interfacial region. In this case, the problem of the interfacial volume is no longer important for copolymer formation. This latter depends very much on the capacities of the PP-*g*-TMI and the microactivator to initiate ϵ-CL. As shown above, the weight percentage of the PP-*g*-PA-6 graft copolymer obtained from the PP-*g*-TMI/ϵ-CL/NaCL/microactivator (50/50/3/3) system was 70.7%. If the amount of the microactivator was zero, one would

then form a pure PP-*g*-PA-6 graft copolymer. It is the capacity of the in situ polymerization and in situ compatibilization process to generate very high amounts of copolymer that allows to reach and stabilize nanodispersion.

Conclusion

We have developed a concept of in situ polymerization and in situ compatibilization for obtaining stabilized nanoblends and shown its feasibility by taking PP/PA-6 blends as example. It consists of polymerizing a monomer of PA-6, ϵ-caprolactam (ϵ-CL), in the matrix of PP. A fraction of the latter bears 3-isopropenyl-α,α-dimethylbenzene isocyanate (TMI) which acts as growing centers to initiate PA-6 chain growth. As such, formation of PA-6 and a PP and PA-6 graft copolymer take place simultaneously in the matrix of the PP, leading to compatibilized nano-PP/PA-6 blends. The size of the particles of the dispersed phase (PA-6) is between 10 and 100 nm, which could not be achieved otherwise by melt blending premade PP and PA-6. Work is under way to further explore the potential of this approach.

Acknowledgment. The authors are very grateful to Borealis, Norway, for its financial and technical support.

References and Notes

(1) Grace, H. P. *Chem. Eng. Commun.* **1982**, *14*, 225.
(2) Elmendorp, J. J. Ph.D. *Thesis*, 1986, TU Delft, The Netherlands.
(3) Nishio, T.; Suzuki, Y.; Kojima, K.; Kakugo, M. *J. Polym. Eng.* **1991**, *10*, 123.
(4) Sundararaj, U.; Macosko, C. W. *Macromolecules* **1995**, *28*, 2647.
(5) Cartier, H.; Hu, G. H. *Polym. Eng. Sci.*, in press.
(6) Hu, G. H.; Cartier, H.; Borve, K. Norway Patent application 1998 (No. 981409); Cartier, H. Ph.D. Thesis, 1997, Université Louis Pasteur de Strasbourg, France.
(7) Kim, K. J.; Kim, Y. Y.; Yoon, B. S.; Yoon, K. J. *J. Appl. Polym. Sci.* **1995**, *57*, 1347.
(8) Greenly, R. A.; Stauffer, J. C.; Kurz, J. E. *Macromolecules* **1969**, *6*, 561.
(9) Vanburskirk, B.; Akkapeddi, M. K. *Polym. Prepr. Am. Chem. Soc., Div. Polym. Chem.* **1988**, *29* (1), 333.
(10) Kye, H.; White, J. L. *Int. Polym. Process.* **1996**, *XI*, 4.
(11) Hergenrother, W. L.; Greenstreet, A. W. (Firestone Tire & Rubber Co) EP 155 *995* (October 1985); *Chem. Abstr. 104*, 7005.
(12) Hornsby, P. R.; Tung, J. F. *Plast. Rubber Composites Process. Appl.* **1995**, *24*, 2.
(13) Matzner, M.; Schober, D. L.; McGrath, J. E. *Eur. Polym. J.* **1973**, *9*, 469.
(14) Matzner, M.; Schober, D. L.; Johnson, R. N.; Robeson, L. M.; McGrath, J. E. *Polym. Sci. Technol.* **1974**, *6*, 125.
(15) Hu, G. H.; Li, H. *J. Polym. Sci., Part A: Chem. Ed.*, Submitted for publication.
(16) Hu, G. H.; Kadri. H. *J. Polym. Sci., Part B: Phys. Ed.* **1998**, *36*, 2153.

MA981924Y